We are IntechOpen,
the world's leading publisher of
Open Access books
Built by scientists, for scientists

4,800
Open access books available

122,000
International authors and editors

135M
Downloads

154
Countries delivered to

Our authors are among the

TOP 1%
most cited scientists

12.2%
Contributors from top 500 universities

WEB OF SCIENCE™

Selection of our books indexed in the Book Citation Index
in Web of Science™ Core Collection (BKCI)

Interested in publishing with us?
Contact book.department@intechopen.com

Numbers displayed above are based on latest data collected.
For more information visit www.intechopen.com

Affinity of CNT for metal – Its importance to application: Molecular dynamics approach

Shuhei Inoue
Hiroshima University
Japan

1. Introduction

As we know, carbon nanotube (especially single-walled carbon nanotube: SWCNT) possesses outstanding properties such as high thermal conductivity, ultra high physical strength, durability, and so forth. Therefore, we expect SWCNT to be a candidate for future material that can realize all of our hopes. However, thinking about its application, the affinity for metal and/or the bonding to metal species are inevitably important problems and those still remain to be unsolved. If there are some discontinuities between SWCNT and metal species, these discontinuities must result in thermal resistance and electrical resistance; that mean we loose the reason and advantage of using SWCNT. If SWCNT can be coated with metal, some new properties may arise, but there is no guarantee that SWCNT can maintain its outstanding properties. These kinds of new approach for application have been partially reported experimentally; however, their mechanisms are not solved. For example, some metal species were deposited on single-walled carbon nanotube forests (Ishikawa et al., 2007) and an isolated single-walled carbon nanotube was coated by metals using e-beam (Zhang et al., 2000). But to investigate the properties of functionalized-SWCNT (metal coated SWCNT) experimentally is extremely difficult. In this chapter molecular dynamics simulation (MD) easily tells us the answers for above-mentioned questions.

The classical MD is merely solving the Newtonian equation according to the forces affected among atoms, but provided the potential function is appropriate, it gives us quite proper perspectives. In this chapter I mention how to build up the appropriate potential function and the coincidence with experimental results of metal deposition on SWCNT. Furthermore, I refer to the perspectives of physical properties of the functionalized-SWCNT.

2. Computational methods

2.1 Driving the potential function

The Brenner potential was applied for carbon-carbon interaction and a classical many-body potential was applied for metal-metal and carbon-metal interactions as a function of the bond order potential. The parameter sets for nickel-nickel and carbon-nickel were derived as a function of coordination number (Shibuta & Maruyama, 2007) while those for gold-gold

atom	S	β (Å^{-1})	D_{e1} (eV)	D_{e2} (eV)	C_D	R_{e1} (Å)	R_{e2} (Å)	C_R	R_1 (Å)	R_2 (Å)
Fe–Fe*	1.3	1.2173	0.4155	0.8392	0.8730	2.627	0	–	2.7	3.2
Ni–Ni*	1.3	1.570	0.4217	1.0144	0.8268	2.4934	0.1096	0.3734	2.7	3.2
Ti–Ti	1.3	2.331	0.6500	0.2001	0.3700	3.819	2.411	0.2357	2.7	3.2
Au–Au	1.3	1.750	0.5290	1.3510	1.5251	3.3043	0.7573	0.2939	2.9	3.5

atom	De (eV)	S	β (Å^{-1})	R_e (Å)	R_1 (Å)	R_2 (Å)	b	δ
Fe–C*	3.3249	1.3	1.5284	1.7304	2.7	3.0	0.0656	-0.4279
Ni–C*	2.4673	1.3	1.8706	1.7628	2.7	3.0	0.0688	-0.5351
Ti–C	3.6240	1.3	1.466	1.8000	2.7	3.0	0.0600	-0.5000
Au–C	2.1840	1.3	2.0745	1.9030	2.9	3.3	0.0970	-0.5350

Table 1. Potential parameters for MD simulations

and carbon-gold were derived by density functional theory (DFT) calculations. Gaussian 03 was employed in this study, and Becke's three-parameter exchange functional with the Lee-Yang-Parr correlation functional (B3LYP) (Beche, 1993 and Lee et al. 1998) was applied. The Los Alamos effective core potential with DZ (LANL2DZ) (Hay et al. 1985) was used as the basis set.

Because the method for deriving parameters is similar to abovementioned paper, it is briefly explained here. First, we assume the symmetrical structure of Au_x and AuC_x clusters that means we do not take into account the Jahn-Teller distortion (Castro et al., 1997) and calculate their total energy. The binding energy is calculated by subtracting isolated energies from the total energy and dividing its result by the number of bonds, as shown in Eq. 1:
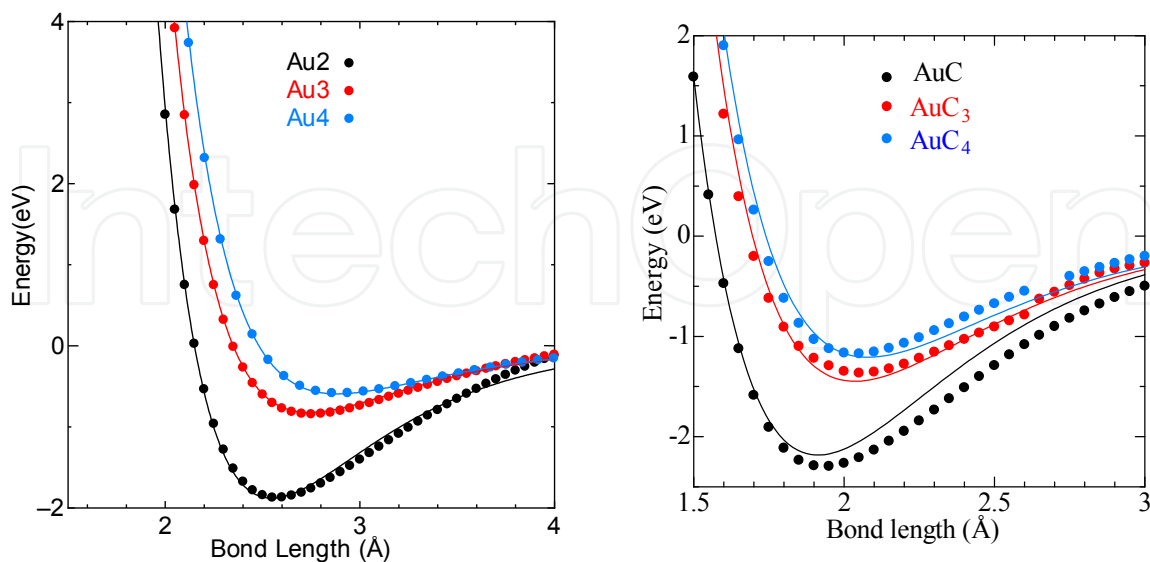

Fig. 1. Fitted potential curves from the lowest ground state derived by DFT calculation (Gaussian03, B3LYP/LANL2DZ). Dots show the binding energies, and the fitted curves are the bond order potential curves. In each case, various spin states are examined and their minimum values are employed.
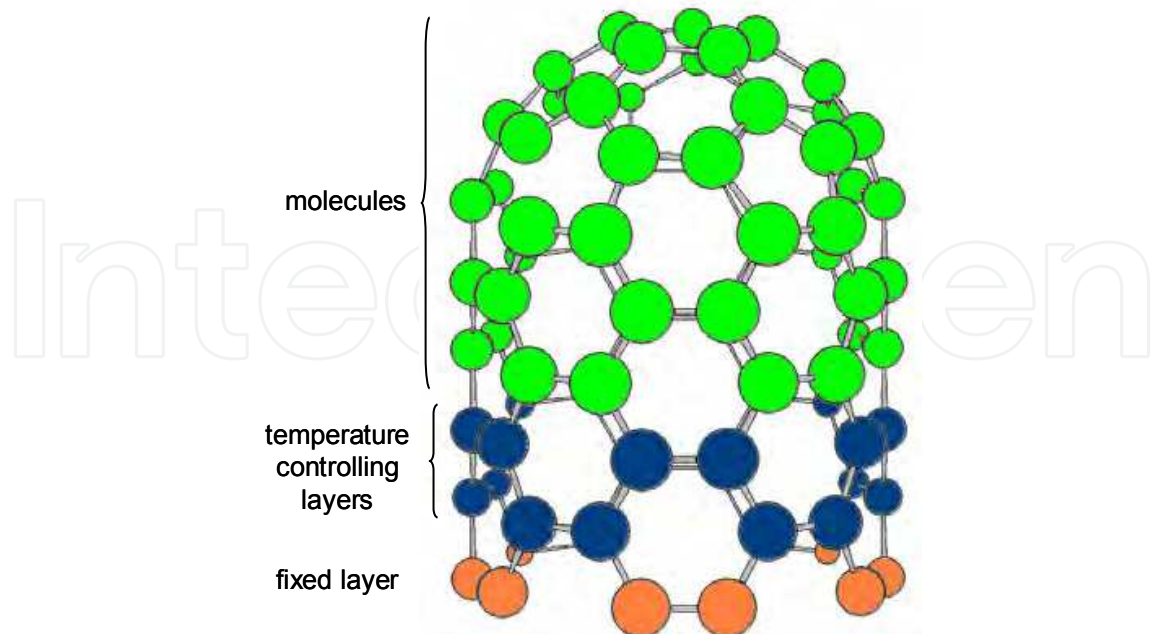
Fig. 2. Surface consisting of a capped carbon nanotube. The calculated system consists of 6 × 6 units (2880 atoms) and has dimensions of 60 Å × 52 Å × 60 Å.

$$De = \left(E_{\min.}^{total} - E_{m,\min.}^{isolated} - N_c \cdot E_{c,\min.}^{isolate}\right)/N_b \qquad (1)$$

where $E_{\min.}^{total}$ denotes the total energy at a certain spin state, $E_{m,\min.}^{isolated}$ is the isolated energy for the metal, N_c is the coordination number of carbon, $E_{c,\min.}^{isolate}$ is the isolated energy for carbon, and N_b is the bond number. In each case, several spin states have been calculated, and their minimum values corresponding to some distance are employed for the fitting. The clusters might take various spin states, but we employ the spin state with the minimum energy. Figure 1 shows the binding energies of gold-gold and carbon-gold derived from DFT calculation and fitted by the potential functions of the bond order potential shown in Eqs. (2–9).
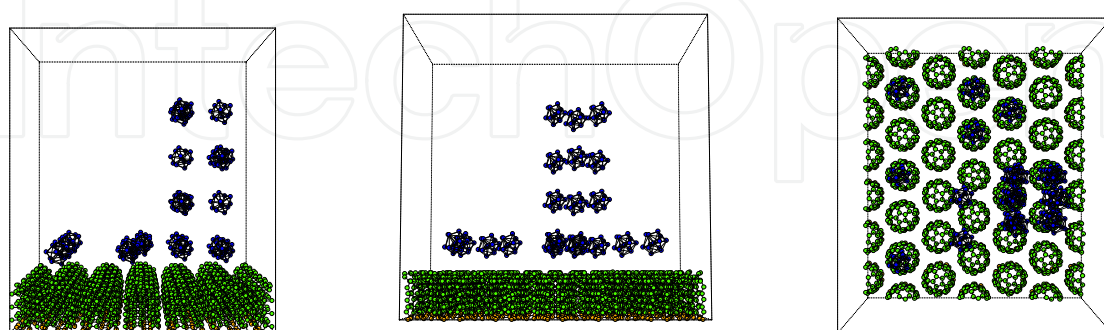
Snapshot from x direction   Snapshot from y direction   Snapshot from z direction

Fig. 3. Cluster configuration onto the flat CNT surface. The center of gravity of each cluster is above the center of the carbon nanotube or its hollow site. To express continuous deposition, some clusters are placed at distances of 10 Å vertically.

$$E = V_R - V_A \tag{2}$$

$$V_R = \frac{D_e}{S-1} \exp\left\{-\beta\sqrt{2S}(r - R_e)\right\} \tag{3}$$

$$V_A = B^* \frac{D_e S}{S-1} \exp\left\{1 + b(N^C - 1)\right\}^\delta \tag{4}$$

$$D_e = D_{e1} + D_{e2} \exp\left\{-C_D(N^M - 1)\right\} \tag{5}$$

$$R_e = R_{e1} - R_{e2} \exp\left\{-C_R(N^M - 1)\right\} \tag{6}$$

$$f(r) = \begin{cases} 1 & (r < R_1) \\ 0.5 \cdot \left(1 + \cos\dfrac{r - R_1}{R_2 - R_1}\pi\right) & (R_1 < r < R_2) \\ 0 & (R_2 < r) \end{cases} \tag{7}$$

$$N_i^C = 1 + \sum_{carbon} f(r_{ik}) \tag{8}$$

$$N_i^M = 1 + \sum_{metal} f(r_{ik}) \tag{9}$$

where r denotes the distance between two atoms and V_R and V_A are the Morse-type potential (Morse, 1929) repulsion and attraction terms, respectively. R_e represents the equilibrium bond length, and D_e is the potential depth at $r = R_e$. S means the ratio of the effective repulsive and attractive terms. N_i^C and N_i^M are the coordination numbers, which are derived by using the cut-off function of $f(r)$. All these parameters are shown in Table 1.

2.2 Physical vapor deposition onto vertically aligned single-walled carbon nanotube

The vertically aligned single-walled carbon nanotube (VA-SWCNT) surface is expressed by a capped short carbon nanotube with a (5, 5) chirality, as shown in Fig. 2. In this paper, the calculated system consists of 6 × 6 units with dimensions of 60 Å × 52 Å × 60 Å, and their configuration resembles the FCC lattice (111). Atoms interact with each other within their cut-off distances. The first layer is a fixed layer, while the second and third layers are temperature-controlling layers. These layers maintain their temperature by velocity scaling. The system has periodic boundary conditions in each direction and the velocity Verlet algorithm is employed. Assuming a realistic metal evaporation in a vacuum chamber, physical vapor deposition (PVD) onto a VA-SWCNT surface is expressed by the collision of each M_{13} cluster with small evaporation energy (kinetic energy, K.E.) of 10.0 meV. Each metal cluster is fully annealed above its melting point (Ni: 1400 K, Au: 1000 K) and set as shown in Fig. 3. The VA-SWCNT is also annealed at 300 K. The melting point of the bulk expressed by these bond order potentials is higher than these temperatures, but the M_{13} cluster is very small and therefore its melting temperature is less than that of the bulk (Ni: 1728 K, Au: 1338 K) (Kittel, 2004).

2.3 Coating nanotube with metal

The dimensions of the calculated system are 60 Å × 100 Å × 100 Å, and a periodic boundary condition is applied in each direction. As shown in Fig. 4, an isolated SWCNT is 60 Å in

Fixed layer

Temperature control layers

60 Å

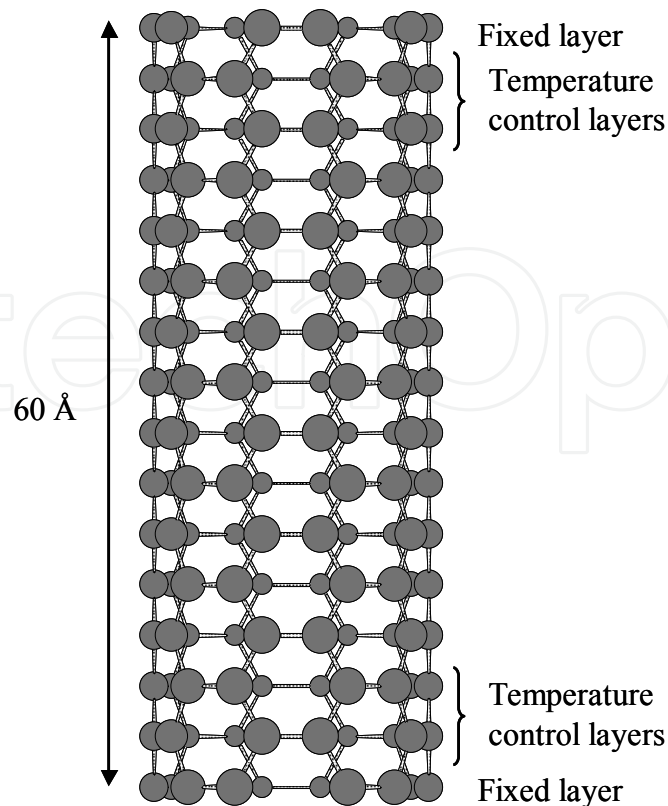Temperature control layers

Fixed layer

Fig. 4. Isolated single-walled carbon nanotube. The both ends are fixed layer and following two layers work to control the temperature.

length with (5, 5) chirality; both its ends are fixed, and the next two layers works to control its temperature. Before coating this carbon nanotube with a metal, it is annealed at 300 K by velocity scaling technique. The molecules of the coating metal are expressed as M_{13} clusters; this expression is suitable for actual experiment because in the conventional metal evaporation process, the average metal particle size is approximately a few angstroms in diameter. This metal cluster is also fully annealed at 1200 – 1400 K; the annealing temperature is clearly higher than their melting temperature but less than their boiling temperature. The melting temperatures in the bulk form expressed by these potential parameters are approximately 1800 – 2000 K; however, in this paper, the metal clusters under study are too small to exhibit bulk properties. In order to achieve continuous metal evaporation coating, the fully annealed metal clusters are distributed at appropriate distances (15 – 20 Å) and made to collide with the carbon nanotube at low evaporation energy of 10 meV or 30 meV.

3. Results and discussion
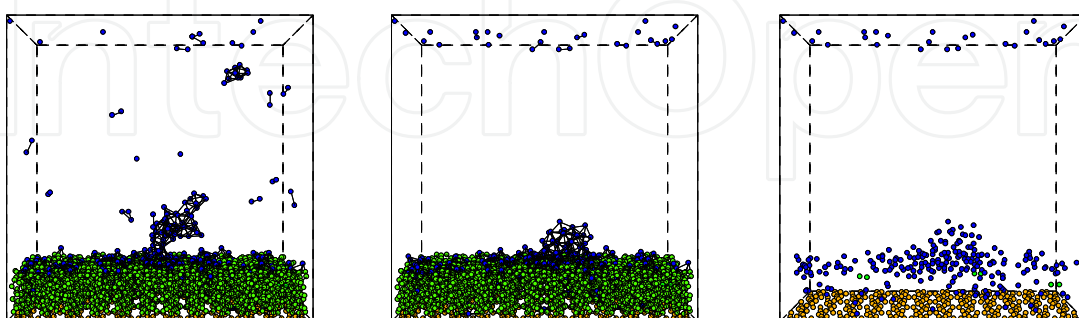
3.1 PVD on VA-SWCNT surface

The initial configuration of the metal clusters is above mentioned and shown in Fig. 3. Each cluster is placed just above the carbon nanotube, or its hollow site for expressing various collision models. In order to express continuous deposition, the clusters are placed at distances of 10 Å. Figure 5 shows the result of PVD onto a VA-SWNTs surface. In both cases,

some of the metal clusters collided with each other before arriving at the surface and formed a larger cluster, while others arrived at the surface without clustering. In the case of nickel deposition, irrespective of clustering, the deposited nickel atoms spread over the VA-SWCNT surface and formed a smooth surface; however, in the case of gold clusters, small clusters of gold could spread over the VA-SWCNT surface, but large clusters could not, and they formed a grain-like structure. On comparing the potential curves of both metals, the equilibrium bond length is slightly different, but the binding energy appears to be almost similar. The point at which they differ the most is the potential depth at which their coordination number is one. The potential depth of gold suddenly decreases as the coordination number increases. This could be a reason for the formation of the grain-like structure, because the contact angle is closely related to the wettability, which is well explained by solid-liquid affinity (ε_{sl} / ε_l) (Maruyama et al., 1998).

According to their results the contact angle tends to become larger as the solid-liquid affinity becomes smaller. In the condensed phase the coordination number should be larger, so that the affinity becomes smaller comparing to that of nickel. The electron configuration of an isolated gold atom is [$4f^{14}$, $5d^{10}$, $6s^1$] and that of a nickel atom is [$3d^8$, $4s^2$]. Therefore, it is speculated that the number of electrons that greatly contribute to binding should be one for gold and more than two for nickel. The order of energy levels of 6s, 4f, and 5d are this order but they are not so far with each other; thus sometimes this order can be reversal for taking a closed shell. In case of gold the 4f-orbit and the 5d-orbit take a closed shell as they
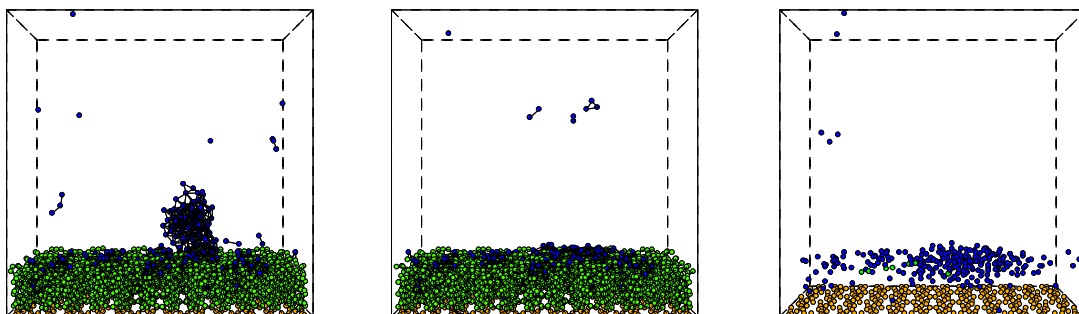
(a) Deposition of nickel clusters.

(b) Deposition of gold clusters.

Fig. 5. Metal PVD onto VA-SCNT surface. In both cases, small metal clusters collide with each other before arriving at the VA-SWCNT surface and form large clusters. The carbon atoms except for those in the fixed layer are hidden in the third figure to identify the metal atoms.

are; therefore, lone electron is one. Thus, the gold atoms have a strong binding energy in the form of a dimmer. On the other hand, the nickel atom has some free electrons, so that their binding energy is smaller than that of the gold atom. Compared to nickel deposition, gold deposition may require stringent conditions to form a flat surface; however, this can be achieved by carrying out deposition under a high vacuum condition and at a low deposition rate. Small clusters of gold can spread over the VA-SWCNT surface, while some of the gold clusters collide with each other before arriving at the surface and form a grain-like structure; it is thus essential to avoid clustering.

3.2 Coating

Figure 6 shows the simulation result of continuous metal evaporation coating ((a) Ti, (b) Fe, (c) Ni, (d) Au). In this simulation, 24 M_{13} clusters were gently collided with one SWCNT. The impact direction was perpendicular to the axis of the carbon nanotube, and at each impact point, about four clusters collided simultaneously. In case of titanium and iron clusters (Fig. 6(a), (b)), the metal atoms seemed to firmly combine with carbon atoms; thus, the metal atoms entered the carbon nanotube and distorted its structure. The strong interaction between the metal atoms and carbon caused the structural deformation of the nanotube; moreover, the continuous impact in a short time for reducing the calculation load (10 ps/layer; usually 1-250 ms/layer in evaporation method for pure gold in experiment) resulted in unrealistic phenomena. In the case of nickel clusters (Fig. 6(c)), the nickel atoms
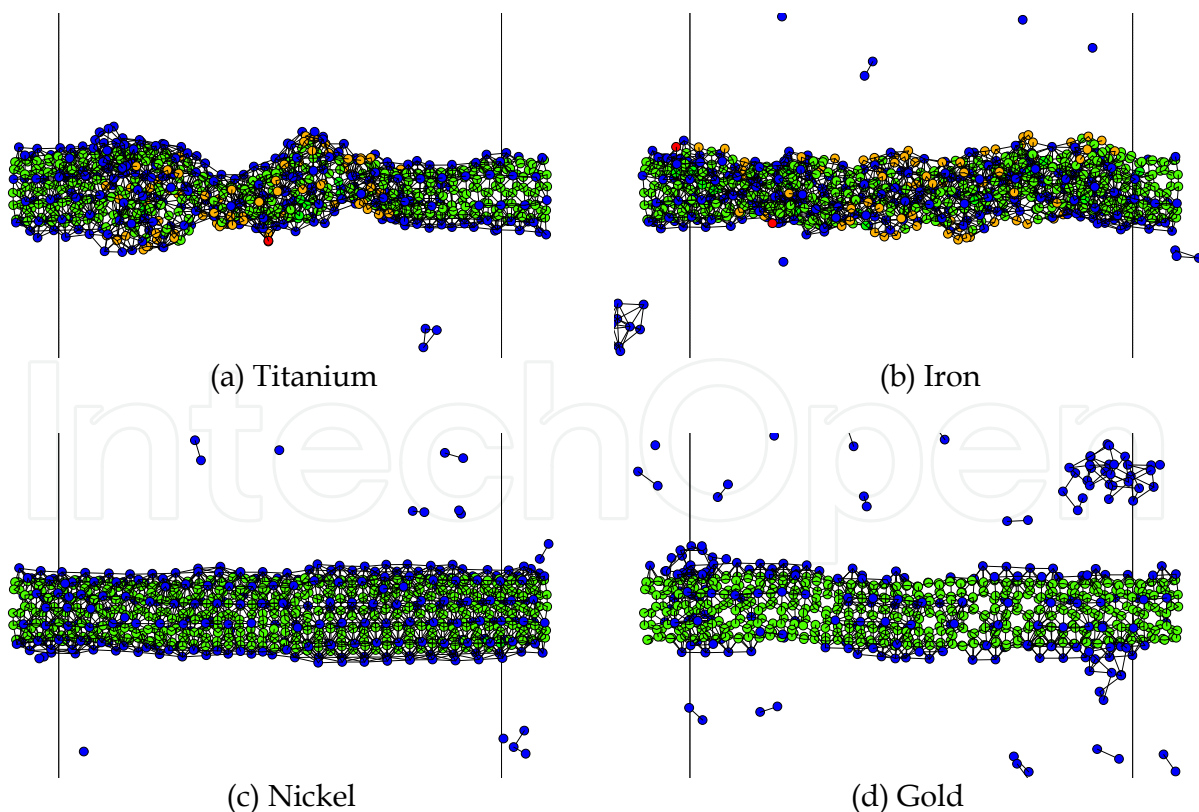

| (a) Titanium | (b) Iron |
| (c) Nickel | (d) Gold |

Fig. 6. Continuous metal evaporation. Blue is metal atom, green is carbon atom with three bonds (sp^2), orange is carbon atom with two bonds (one dangling bond), and red is carbon atom with one bond (two dangling bonds).

smoothly and seamlessly covered the carbon nanotube. The equilibrium position of the nickel atoms coincided with the center of the hexagonal carbon network. When the first nickel cluster collided with the carbon nanotube, a grain structure was temporarily formed; however, the nickel atoms immediately found a stable position and moved into it. Once they reached the equilibrium position, they remained stationary at this temperature. Next, the second cluster reached the surface, acquired a grain structure instantly, and then moved to the most stable site. When all the clusters reached the surface, the equilibrium position on the carbon network was saturated; therefore, the nickel clusters formed a second metal layer on the carbon nanotube. Even at this stage, the nickel atoms did not form a grain structure but formed a smooth and seamless layer. Figure 6(d) shows the result of gold cluster coating. According to Zhang et al., gold atoms form a grain structure and exhibit a highly discontinuous coating; however, according to our simulation, the gold atoms can be coated smoothly but discontinuously. The gold atoms initially formed a grain structure, as reported by Zhang et al.; this was because the gold clusters were accidentally concentrated in the same area on the carbon nanotube. This indicates that if the evaporation rate decreases or the experiment is conducted under a higher vacuum condition, the formation of a grain structure can be avoided. Zhang et al. explained this result in terms of the weak interaction between the gold atoms and the SWCNT. However, according to our DFT calculations, the binding energy of the Au-C bond is not low; on the contrary, it is slightly larger than the binding energy of the Au-Au bond. The value of the binding energy is not considered to be significant; however, the ratio of the binding energies, i.e., $\varepsilon_{M\text{-}C}$ / $\varepsilon_{M\text{-}M}$, should be substantial. Because these condition each atom has many coordination number, the values of this ratio for titanium, iron, nickel, and gold are 2, 3, 1.5 (approximately), and 1 (approximately), respectively. Thus, in the case of titanium and iron coating, the carbon atoms experience an outward pull and the nanotube structure gets deformed. In the case of nickel, a very smooth coating is achieved. On the other hand, in the case of gold, though the Au-C interaction is slightly stronger than the Au-Au interaction, a grain structure is formed. In some areas, the gold atoms are deposited smoothly but not seamlessly. The reason for this phenomenon is attributed to the equilibrium bond length. As mentioned above, the most stable site for the first layer metal atoms is the center of the hexagonal carbon network, of which diameter is 2.5 Å. Coincidently, the equilibrium bond lengths of nickel and iron are comparable, but that of gold is slightly greater (2.6-3.3 Å, depending on the coordination number). The gold atoms must have a shorter bond length so that they can get accommodated in the stable site of the carbon nanotube, thereby creating a discontinuous coating that reduces the distortion energy. Thus, even gold atoms can be coated smoothly, provided the distances between them is sufficient to reduce the distortion for each fragment of coating (in our simulation, the fragment of coatings is approximately 10-15 nm in length). Owing to the strong C-Ti and C-Fe interactions, the structure of the carbon nanotube is distorted under a high coating rate in our simulation. In order to confirm this, a lower coating rate is applied and the results are examined. In this case, each M_{13} cluster collides with the center of the carbon nanotube in a sequence. For the fully annealing, this sequential impact took an enough interval. Figure 7 shows this sequential impact of the metal clusters on the carbon nanotube. A full annealing duration for each impact step results in a smooth and continuous coating and no defects are observed in the carbon nanotube. A schematic diagram of the iron cluster impact is shown in Fig. 3(a). Similar to the nickel atom, the iron atom finds a stable position and moves into it. However, in this simulation, because each
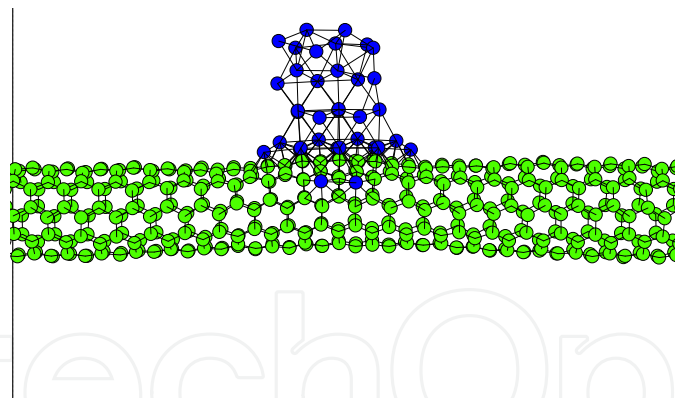
cluster reaches almost the same position, all the iron atoms do not spread over the surface
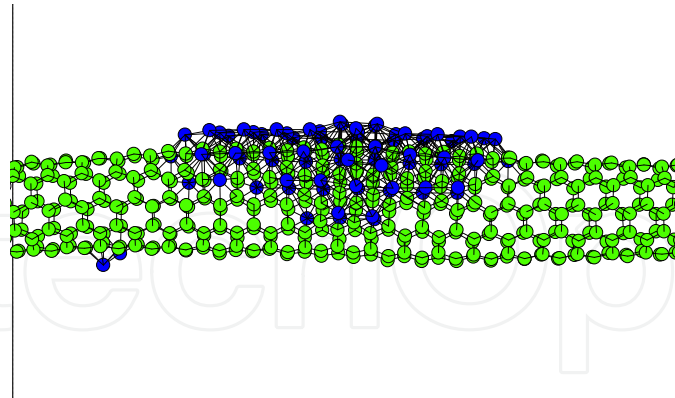
(a) Sequential Fe coating. Totally six Fe_{13} clusters collide.
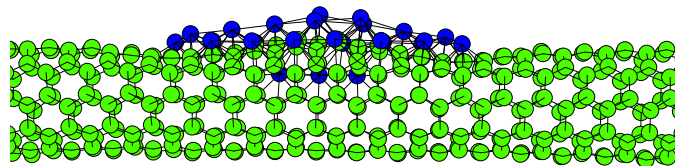
(b) Sequential Ti coating. Totally three Ti_{13} clusters collide.

(c) Sequential Au coating. Totally three Au_{13} clusters collide.

Fig. 7. Sequential impacts of Fe, Ti, and Au cluster on the carbon nanotube surroundings with enough annealing duration after every impact.

but form a second layer. This can occur in the nickel system as well. When too many clusters arrive at the same point, each atom seeks the stable site and tends to move into it, but the temperature reduces before the diffusion is completed. As a result, the iron atoms form a second layer. A similar behavior is observed in titanium coating, as shown in Fig. 7 (b). However, in the case of titanium clusters, when the impact energy is small, a different phenomenon is observed. In our simulation, first three clusters were able to reach the

surface even at a low evaporation energy, but the next cluster could notreach. This can be attributed to the difference in the equilibrium bond lengths. According to Eq. 6, if the number of coordinates is sufficient, the equilibrium bond length must be equal to R_{e1} for the metal-metal potential and the metal-carbon equilibrium bond length is simply determined as a function of R_e (Table 1). A comparison reveals that the difference in this value for the titanium coating system are larger than those for the iron coating system. This is because if there is a titanium layer on the carbon nanotube, the cluster having a small impact energy cannot overcome the repulsive energy. Thus, the cluster is reflected before it is attracted to the carbon atoms.

This proves that at a high evaporation energy (e.g., 1 eV), the titanium cluster can arrive at the surface and produce a smooth coating. This might be a reason why the titanium coating is smoother than the nickel coating in the experimental results. [15] In the case of gold coating, as shown in Fig. 6(c), the first cluster was able to spread over the surface but the second and the third could not; therefore, they formed a grain structure. This indicates that if the gold cluster reaches the same place, as in the case of the experiment with a high deposition rate, the grain formation is not avoidable, as inferred from Fig. 7(d). From the point of wettability the contact angle is closely related to the wettability, which is mentioned above section explained by solid-liquid affinity (ε_{sl} / ε_l). According to their results the contact angle tends to become larger as the solid-liquid affinity becomes smaller that means the gold cluster tends to form a grain structure.

3.3 Physical properties

Figure 8 shows the stress-strain (force-strain) curves of coated and uncoated SWCNT. In this simulation one end of SWCNT was fixed and the other end was pulled slowly enough to be annealed that avoid unintentionally breaking of SWCNT. Owing to the disturbance of perfect sp^2 bonding of SWCNT, it might be easily expected that the physical strength becomes much weaker, but the decrease is not so large; or rather, the force constant becomes larger. The rupture is induced by metal atom that tends to take the bonds from the carbon. Because the bond length of carbon-metal is longer than that of carbon-carbon, the interaction between carbons becomes suddenly weaker than that of carbon-metal when the SWCNT pulled.

Figure 9 indicates the thermal diffusivity of coated and uncoated SWCNT. The thermal diffusivity is derived by fitting the one-dimensional non-Fourier heat conduction equation with two relaxation timescales (τ_1, τ_2) shown below equation.

$$\tau_1 \frac{\partial^2 T}{\partial t^2} + \frac{\partial T}{\partial t} = \alpha \left(\nabla^2 T + \tau_2 \frac{\partial}{\partial t} \nabla^2 T \right) \tag{10}$$

The dominant heat carrier in SWCNT is phonon and this equation model is fully described in other's paper (Shiomi & Maruyama, 2006).
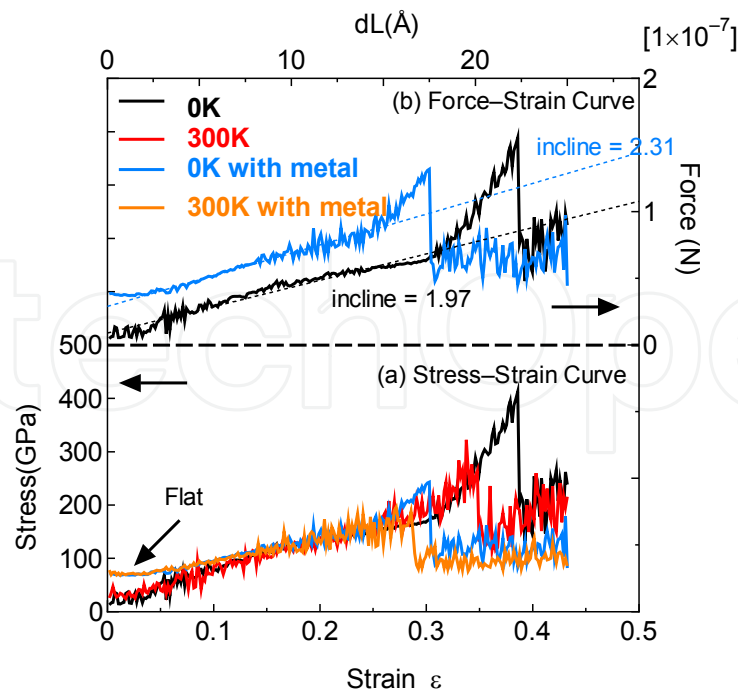
Fig. 4

Fig. 8. The stress–strain curve (a) and force–strain curve (b). The stress is defined by assuming their cross section with 6.93 Å for the uncoated SWCNT and 8.32 Å for the metal-coated SWCNT in diameter. The metal-coated SWCNT meets earlier rupture point but has a larger force constant. The metal-coated SWCNT has a residual stress that makes the inclination flat in a small strain (displacement) range.
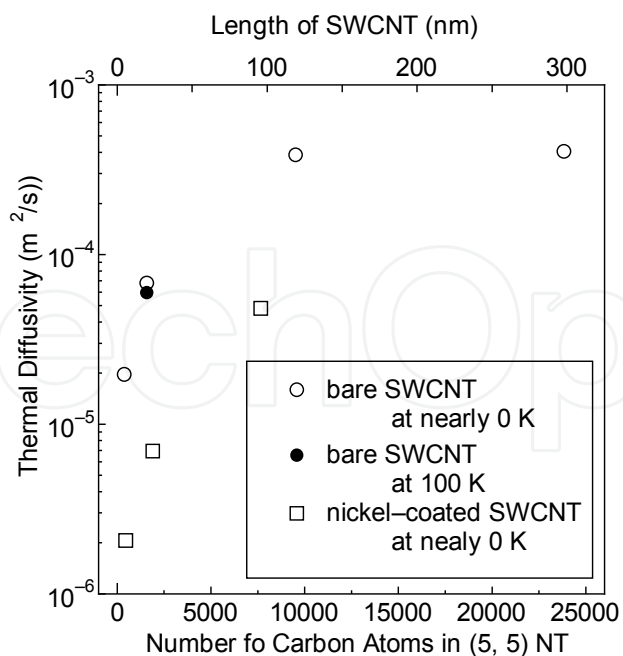

Fig. 9. Thermal diffusivity estimated in this study. The thermal diffusivity of the nickel-coated SWCNT decreases by 90%. The estimated thermal conductivity (λ) is expressed as follows: $\lambda = 1 \times 10^6 \, \alpha - 3 \times 10^6 \, \alpha$. It depends on the definition of the density and specific heat capacity (C_v) of the SWCNTs is assumed to be $3R$, where R is a gas constant.

4. Conclusion

In this chapter MD approach for CNT analysis was explained. The classical MD merely solves the Newtnian equation, but if the potential function is fully appropriate, the results must be convincive. In case of PVD and coating this simulation shows good agreement with the experimental results; on the other hand, for the physical properties, the adequate results are given and also the mechanism should become clear.

5. References

Beche AD. (1993) Density-Functional Thermochemistry .3. The Role of Exact Exchange. *J. Chem. Phys.* 98, 1993, 5648-5652.

Castro M, et al. (1997) Structure, bonding, and magnetism of small Fe-n, Co-n, and Ni-n, clusters, n<=5. *Chem. Phys. Lett.* 271 1997, 133-142.

Hay PJ & Wadt WR. (1985) Abinitio Effective Core Potentials for Molecular Calculations - Potentials for the Transition-Metal Atoms Sc to Hg. *J. Chem. Phys.* 82, 1985, 270-283.

Ishikawa K. et al. (2007) Extended abstracts, ASME-JSME Thermal Eng., (2007) HT2007-32783.

Kittel C. (2004)Introduction to Solid State Physics. John Wiley & Sons Inc. 2004.

Lee CT, et al. (1998) G. Development of the Colle-Salvetti Correlation-Energy Formula Into a Functional of the Electron-Density. *Phys. Rev. B* 37, 1998, 785-789.

Maruyama S. et al. Liquid droplet in contact with a solid surface. *Micro Thermophys. Eng.* 2, 1998, 49-62.

Morse PM. (1929) Diatomic Molecules According to the Wave Mechanics. II. Vibrational Levels. *Phys. Rev.* 34, 1929, 57-64.

Shibuta Y, Maruyama S. (2007) Bond-order potential for transition metal carbide cluster for the growth simulation of a single-walled carbon nanotube. *Comput. Mat. Sci.* 39, 2007, 842-848.

Shiomi J & Maruyama S. (2006) Non-Fourier heat conduction in a single-walled carbon nanotube: Classical molecular dynamics simulations. , 273 2006, 205420.

Zhang Y. et al. *Phys. Lett.*, 331 (2000) 35.

Carbon Nanotubes

Edited by Jose Mauricio Marulanda

This book has been outlined as follows: A review on the literature and increasing research interests in the field of carbon nanotubes. Fabrication techniques followed by an analysis on the physical properties of carbon nanotubes. The device physics of implemented carbon nanotubes applications along with proposed models in an effort to describe their behavior in circuits and interconnects. And ultimately, the book pursues a significant amount of work in applications of carbon nanotubes in sensors, nanoparticles and nanostructures, and biotechnology. Readers of this book should have a strong background on physical electronics and semiconductor device physics. Philanthropists and readers with strong background in quantum transport physics and semiconductors materials could definitely benefit from the results presented in the chapters of this book. Especially, those with research interests in the areas of nanoparticles and nanotechnology.

How to reference

In order to correctly reference this scholarly work, feel free to copy and paste the following:

Shuhei Inoue (2010). Affinity of CNT for Metal - Its Importance to Application: Molecular Dynamics Approach, Carbon Nanotubes, Jose Mauricio Marulanda (Ed.), ISBN: 978-953-307-054-4, InTech, Available from: http://www.intechopen.com/books/carbon-nanotubes/affinity-of-cnt-for-metal-its-importance-to-application-molecular-dynamics-approach

INTECH
open science | open minds